Leptin Receptor^{+} cells create a perisinusoidal niche for thrombopoiesis in the bone marrow by synthesizing CXCL14

Yuanyuan Xue[1], Salma Merchant[1], Amanda Reyes[1], Maowu Luo[2], Ruixuan Zhang[1], Trevor Tippetts[1], Gerik Grabowski[1], Tai Ngo[3], Yanan Zhang[4], Zhiguo Shang[3], Nisi Jiang[1], Elise Jeffery[1], Yafeng Li[1], Tao Wei[1], Wen Gu[1], Liming Du[1], Ralph J. DeBerardinis[1,5,6], Kevin M. Dean[3], Thomas P. Mathews[1], Daniel Lucas[4], Zhiyu Zhao[1], Sean J. Morrison[1,5]

[1] Children's Research Institute and the Department of Pediatrics, University of Texas Southwestern Medical Center, Dallas, TX, USA.

[2] Department of Pathology, University of Texas Southwestern Medical Center, Dallas, TX, USA

[3] Lyda Hill Department of Bioinformatics, University of Texas Southwestern Medical Center, Dallas, TX, USA

[4] Division of Experimental Hematology and Cancer Biology, Cincinnati Children's Medical Center, Cincinnati, OH, USA

[5] Howard Hughes Medical Institute, UT Southwestern Medical Center, Dallas, TX, USA

[6] The Eugene McDermott Center for Human Growth and Development, UT Southwestern Medical Center, Dallas, TX, USA

Corresponding author: Sean J. Morrison, sean.morrison@utsouthwestern.edu, (214)648-2352

Data sharing statement: For original data, contact Sean.Morrison@UTSouthwestern.edu

Data and code availability

All data reported in this paper will be shared by the lead contact upon reasonable request. The RNA sequencing data generated in this paper have been deposited at the Sequence Read Archive BioProject ID PRJNA1225166. Source code related to the analysis of single-cell RNA sequencing, bulk RNA sequencing, and lipidomics data analysis can be found at https://git.biohpc.swmed.edu/CRI/morrison-lab/scRNASeq, https://git.biohpc.swmed.edu/CRI/morrison-lab/RNASeq, and https://git.biohpc.swmed.edu/CRI/ODA, respectively. Any additional information required to reanalyze the data reported in this paper is available from the lead contact upon request.

Materials availability

A material transfer agreement is required to obtain *Cxcl14*^{flox} or *Cxcl14*^{dsRed} mice in accordance with the regulations of the University of Texas Southwestern Medical Center.

Key points

- Leptin Receptor^{+} stromal cells regulate terminal differentiation in megakaryocytes in addition to maintaining stem and progenitor cells
- CXCL14 from Leptin Receptor^{+} cells promotes the formation of platelets by remodeling lipid metabolism in megakaryocytes in the bone marrow

Abstract

Leptin Receptor-expressing (LepR$^+$) stromal cells in the bone marrow are a critical source of growth factors for the maintenance of hematopoietic stem cells (HSCs) and most restricted hematopoietic progenitors. An important unresolved question is whether they also regulate terminal differentiation in some hematopoietic cells. We found that LepR$^+$ cells promote thrombopoiesis by synthesizing the chemokine CXCL14, which is expressed in the bone marrow by a subset of LepR$^+$ cells. *Cxcl14*-expressing LepR$^+$ cells extend fine processes that wrap around perisinusoidal megakaryocytes. Deletion of *Cxcl14* from LepR$^+$ cells did not significantly alter HSC function or most aspects of bone marrow hematopoiesis, including megakaryocyte generation; however, it significantly reduced the numbers of proplatelet-forming megakaryocytes in the bone marrow and platelets in the blood. CXCL14 promoted platelet formation by remodeling lipid metabolism in megakaryocytes, increasing fatty acid transporter expression and enabling megakaryocytes to use more polyunsaturated fatty acids from the circulation. A high fat diet rescued the formation of proplatelet-forming megakaryocyte and platelets in *Lepr-cre; Cxcl14* $^{fl/fl}$ mice. CXCL14 protein was sufficient to promote platelet formation by megakaryocytes in vitro and in vivo. LepR$^+$ cells thus create a perisinusoidal niche for thrombopoiesis by producing CXCL14, which regulates lipid metabolism and terminal differentiation in megakaryocytes.

INTRODUCTION

Leptin Receptor-expressing (LepR$^+$) stromal cells promote the maintenance of hematopoietic stem cells (HSCs) and most restricted hematopoietic progenitors in the bone marrow by producing Stem cell factor (SCF)[1-3], CXCL12[4,5], Pleiotrophin[6], Interleukin 7 (IL7)[7], and colony stimulating factor 1 (CSF1)[8-10]. LepR$^+$ cells have also been described as CXCL12-abundant reticular (CAR) cells[11,12]. Some LepR$^+$ cells are perisinusoidal, where they create niches for HSCs, erythroid progenitors, and other restricted hematopoietic progenitors[1,2,4,13-15]. Other LepR$^+$ cells are peri-arteriolar, where they create niches for lymphoid progenitors[16]. LepR$^+$ cells also promote vascular regeneration by producing Angiopoietin-1[17] and VEGF-C[18] as well as peripheral nerve maintenance in bone marrow by producing nerve growth factor[19]. However, it is unknown whether LepR$^+$ cells regulate terminal differentiation in any hematopoietic cells.

Platelets regulate hemostasis, inflammation, and tissue repair by enabling blood clotting[20]. Platelets are produced in the bone marrow by megakaryocytes[21,22], which localize to sinusoidal blood vessels[23,24] and release platelets into circulation[25]. A number of cytokines promote the formation of megakaryocytes in the bone marrow including thrombopoietin[26-28], SCF[29-31], leukemia inhibitory factor[32], fibroblast growth factor 4[33,34], IL-3, IL-6 and IL-11[29,35-38]. Thrombopoietin is produced by hepatocytes in the liver[39] and SCF is produced by LepR$^+$ cells in the bone marrow[1] but the cellular sources of other factors are uncertain. The migration of megakaryocytes to sinusoids may be mediated by CXCL12 made by LepR$^+$ cells[40,41].

Megakaryocytes differentiate from HSCs as well as from restricted progenitors that arise from multipotent progenitors[42-47]. Several cytokines and chemokines promote the maturation of megakaryocytes into proplatelet-forming megakaryocytes or the generation of platelets including Insulin growth factor 1[48], IL-1a[49], chemokine ligand 5[50], and Interferon alpha (IFNα)[51]. IFNα is produced by plasmacytoid dendritic cells in the bone marrow[51] but to our knowledge the cellular sources of other cytokines and chemokines are uncertain.

CXCL14 is a chemokine that is highly conserved between humans and mice and expressed in multiple tissues[52], including in bone marrow stromal cells[53] and platelets[54]. CXCR4, which is ubiquitously expressed by hematopoietic cells, serves as a receptor for CXCL14[54,55], though there may also be other receptors[56-59]. CXCL14 promotes immune cell migration to sites of inflammation[60,61] as well as platelet migration and thrombus formation[54]. CXCL14 expression is lost from the bone marrow in chronic myeloid leukemia and this contributes to imatinib resistance[53]. However, CXCL14 has not been shown to play any role in the regulation of hematopoiesis or thrombopoiesis.

METHODS

Mice

All mice were maintained on a C57BL/6 background. *Scf*^{GFP} (*Kitl*$^{tm1.1Sjm}$; a GFP knockin allele that reports *Scf* expression) was generated in our laboratory. *Lepr*^{cre} (B6.129(Cg)-Lepr$^{tm2(cre)Rck}$; a Cre allele expressed by *Lepr*$^{+}$ cells)[62] was obtained from Jackson Laboratory. *Prx1-cre* (B6.Cg-Tg(Prrx1-cre)1Cjt; a Cre allele expressed by limb mesenchymal cells)[63]. *Cxcl14*^{dsRed} and *Cxcl14*^{flox} mice were generated in this study. Male and female mice were used in most experiments. C57BL/Ka-Thy-1.1/ C57BL/Ka-Thy-1.2 (CD45.2/CD45.1) mice or C57BL/Ka-Thy-1.2 (CD45.1) mice were used as recipients or as a source of competitor bone marrow cells in transplantation experiments. Recipient mice were given Baytril (0.1 mg/ml in the drinking water) for 1 week prior to, and one month after, irradiation.

To generate the *Cxcl14*^{flox} and *Cxcl14*^{dsRed} mice, Alt-R S.p. Cas9 Nuclease V3 (Integrated DNA Technologies), sgRNA (Synthego, Supplemental Table S6), tracrRNAs and donor oligos (Azenta, Supplemental Table S6) were microinjected into C57BL/6 zygotes. Chimeric mice were genotyped by sequencing the targeted locus, confirming the correct insertion of loxP or dsRed sequences, and then by PCR analysis. Founders were backcrossed with C57BL/Ka mice for at least three generations prior to analysis.

Mice were housed in the Animal Resource Center at UT Southwestern in a specific-pathogen-free facility under a 12 h:12 h light:dark cycle with a temperature of 18–24 °C and humidity of 35–60%. For experiments with high-fat diets, 4-5 month-old control and *Lepr-cre; Cxcl14*$^{fl/fl}$ mice were placed on the following diets: normal chow (Research Diets, D12450Ji), HFD1 diet (Research Diets, D22050405i), HFD2 diet (Research Diets, D12492i). All procedures were approved by the UT Southwestern Institutional Animal Care and Use Committee.

Lipid extraction and lipidomic data analysis

Bone marrow megakaryocytes were transferred to glass vials for Bligh-Dyer lipid extraction using methanol:PBS:chloroform (1:1:2) containing 0.1% formic acid. Mass spectrometry was performed as described[64]. Positive and negative lipid intensity data from the experiments were combined, normalized using the relative log expression (RLE) method[65] and log-transformed. Lipid species that significantly differed among treatments (log2 fold change > 0.5 in either direction and false discovery rate (FDR) < 0.05) were identified using Omics Data Analyzer (ODA) V2.2[66] with generalized linear modelling, taking batch effects into account.

Measuring fatty acid uptake in vivo using $^{13}C_{18}$-linoleic acid

Jugular catheters were implanted in *Lepr-cre; Cxcl14*$^{fl/fl}$ and control mice. After a week of recovery, the mice were fasted for 4 hours, infused intravenously with $^{13}C_{18}$-linoleic acid conjugated to BSA for 24 hours, then blood and bone marrow were collected. CD42d^{+} megakaryocytes were isolated from bone marrow using paramagnetic beads, then lipids were extracted and analyzed by LC/MS/MS[58]. We calculated the theoretical mass of isotopically labeled lipid species as described[67] then used these values to derive a library of isotopically labeled lipid species that included phospholipids, triglycerides, and free fatty acids. Lipidomic data were searched against this library with 5 ppm mass accuracy. Peaks that appeared to be

isotopically labeled versions of lipids were confirmed through MS/MS analysis. All data was corrected for naturally abundant isotopes and the fractional enrichments and pool sizes of each lipid were quantified.

Recombinant mouse CXCL14 treatment

Recombinant mouse CXCL14 (R&D, Catalog #: 730-XC) was intravenously injected into mice at a dose of 20 µg/kg body weight in a volume of 150 µl per mouse. The equivalent volume of sterile PBS was injected into control mice. The mice were analyzed 16 hours after injection.

Additional methods can be found in Supplementary Materials.

RESULTS

***Cxcl14* is mainly expressed by LepR$^+$ cells in bone marrow**

To assess the *Cxcl14* expression pattern in the bone marrow, we reanalyzed published single cell RNA sequencing data from enzymatically dissociated bone marrow cells[68]. *Cxcl14* was strongly expressed by LepR$^+$ cells but rarely by osteoblasts, chondrocytes, fibroblasts, arteriolar endothelial cells, sinusoidal endothelial cells, pericytes, or Schwann cells (Figure 1A). Quantitative reverse transcription PCR (qRT-PCR) confirmed *Cxcl14* was expressed by LepR$^+$CD45$^-$Ter119$^-$CD31$^-$ stromal cells but was not detected in endothelial cells, HSCs or WBM cells (Figure 1B). *Cxcl14* was expressed by both *Osteolectin* negative *Lepr*$^+$ cells, which are perisinusoidal[1], and *Osteolectin*$^+$*Lepr*$^+$ cells, which are peri-arteriolar[16] (Figure 1A).

To further analyze the *Cxcl14* expression pattern in adult bone marrow, we generated a *Cxcl14*-dsRed (*Cxcl14*^{dsRed}) knock-in reporter allele (Supplemental Figure1A-B). Deep confocal imaging[15] of femurs from adult *Cxcl14*$^{dsRed/+}$*; Scf*$^{GFP/+}$ mice showed *Cxcl14*^{dsRed} expression by perisinusoidal and peri-arteriolar stromal cells (Figure 1C-E). The peri-arteriolar *Cxcl14*^{dsRed} cells were particularly noticeable near the endosteum as well as in the central marrow while the

perisinusoidal *Cxcl14* ^{dsRed} cells were throughout the bone marrow (Figure 1C). The *Cxcl14* ^{dsRed}-expressing perisinusoidal stromal cells were *Scf*-GFP^{+} (Figure 1D) and LepR^{+} (Figure 1E).

Flow cytometric analysis of enzymatically dissociated bone marrow cells from adult *Cxcl14* $^{dsRed/+}$*; Scf* $^{GFP/+}$ mice showed that *Cxcl14* ^{dsRed} was expressed by 0.19±0.045% of bone marrow cells, 91±0.85% of which were LepR^{+} (Figure 1F). Furthermore, 89±1.5% of LepR^{+} cells were *Cxcl14* ^{dsRed} positive (Figure 1G). The vast majority of *Cxcl14* ^{dsRed} positive cells were also positive for *Scf*-GFP (Figure 1H). We rarely detected *Cxcl14* ^{dsRed} expression by endothelial cells (Figure 1I) or hematopoietic cells in the bone marrow (Figure 1J; Supplemental Figure 1C). The flow cytometry gates used to sort LepR^{+} cells and endothelial cells are in Figure 1G-I and the gates for hematopoietic cells are in Supplemental Figure 1D-G.

CXCL14 is required for thrombopoiesis but not megakaryopoiesis

To test if CXCL14 regulates hematopoiesis, we generated mice with a floxed *Cxcl14* allele by inserting loxp sites on either side of exon 2 (Supplemental Figure 2A-B). Cre mediated recombination would be predicted to yield a strong loss of CXCL14 function as deletion of exon 2 causes a frameshift. *Lepr-cre; Cxcl14* $^{fl/fl}$ mice were born in expected numbers and did not significantly differ from littermate controls in terms of gross appearance (Supplemental Figure 2C) or body mass (Supplemental Figure 2D). Using qRT-PCR primers that amplified the deleted sequence, we found that LepR^{+} cells had substantially lower levels of *Cxcl14* transcripts in 4 month-old *Lepr-cre; Cxcl14* $^{fl/fl}$ mice as compared to littermate controls (approximately 30% of control levels; Supplemental Figure 2E). This indicated that *Cxcl14* was deleted in most LepR^{+} cells by 4 months of age.

Four month-old *Lepr-cre; Cxcl14*$^{fl/fl}$ and littermate control mice did not significantly differ in terms of bone marrow cellularity (Figure 2A) or the frequencies of HSCs (Figure 2B), MPPs (Figure 2C), restricted hematopoietic progenitors (Figure 2D-P), or differentiated myeloid, B, T, or megakaryocyte lineage cells (Figure 2Q-U) in the bone marrow. They also did not

significantly differ in terms of spleen cellularity (Supplemental Figure 2F) or the frequencies of HSCs, MPPs, restricted progenitors, or differentiated hematopoietic cells in the spleen (Supplemental Figure 2G-Y). Finally, *Lepr-cre; Cxcl14*$^{fl/fl}$ and littermate control mice did not significantly differ in the reconstituting potential of bone marrow cells upon competitive transplantation into irradiated mice (Supplemental Figure 2Z) or the frequencies of bone marrow or spleen cells that formed colonies in culture, including megakaryocyte colonies (Supplemental Figure 2AA-AD). CXCL14 is thus not required for HSC maintenance, HSC function, or bone marrow hematopoiesis, including the generation of megakaryocytes.

Four month-old *Lepr-cre; Cxcl14*$^{fl/fl}$ and littermate control mice did not significantly differ in terms of white blood cell (WBC) or red blood cell (RBC) counts but *Lepr-cre; Cxcl14*$^{fl/fl}$ mice had significantly lower platelet counts (Figure 2V; 20% reduction). By 7 months of age, this phenotype was more severe as *Lepr-cre; Cxcl14*$^{fl/fl}$ mice exhibited a 37% reduction in platelet counts, with normal WBC and RBC counts (Figure 2W). Even at 4 months of age, the reduction in platelet counts was associated with prolonged bleeding in *Lepr-cre; Cxcl14*$^{fl/fl}$ as compared to control mice when their tails were severed 1 mm from the end (Figure 2X). Therefore, CXCL14 expression by LepR^{+} cells was required for normal platelet production despite not being required for normal HSC function or other aspects of hematopoiesis.

To test if CXCL14 promotes platelet regeneration we depleted platelets by injecting mice with anti-CD42b antibody[51] or by sublethally irradiating. In both cases, *Lepr-cre; Cxcl14*$^{fl/fl}$ and control mice did not significantly differ in terms of WBC or RBC counts but platelet regeneration was significantly delayed in *Lepr-cre; Cxcl14*$^{fl/fl}$ mice (Figure 2Y and 2Z).

Cxcl14 from LepR^{+} cells promotes the formation of proplatelet-forming megakaryocytes

Megakaryocytes grow in size and mature into proplatelet-forming megakaryocytes that extend processes into sinusoidal blood vessels to shed platelets into circulation[22]. Based on confocal imaging of cleared femurs, *Lepr-cre; Cxcl14*$^{fl/fl}$ and control bone marrow did not

significantly differ in terms of the numbers of all CD41$^+$ megakaryocytes (Figure 3A-B) but the megakaryocytes in control bone marrow were significantly larger (Figure 3C) and included more proplatelet-forming megakaryocytes (Figure 3D). We did not observe a significant difference in DNA content between CD42d$^+$ megakaryocytes analyzed by flow cytometry from the bone marrow of *Lepr-cre; Cxcl14*$^{fl/fl}$ and control mice (Supplemental Figure 3A-B); however, it is possible that the most mature megakaryocytes were excluded from this analysis as they would have been too large to analyze by flow cytometry.

We also analyzed sections through mature megakaryocytes in the bone marrow of *Lepr-cre; Cxcl14*$^{fl/fl}$ and control mice by transmission electron microscopy (Figure 3E). During their maturation, megakaryocytes form a demarcation membrane system that envelops developing platelets in the cytoplasm. We observed a significant reduction in demarcation membranes within megakaryocytes from the bone marrow of *Lepr-cre; Cxcl14*$^{fl/fl}$ as compared to control mice (Figure 3E-F), indicating impaired megakaryocyte maturation[69,70]. CXCL14 from LepR$^+$ cells was, thus, not required for the formation of megakaryocytes but was required for their maturation into proplatelet-forming megakaryocytes.

We assessed the localization of megakaryocytes and proplatelet-forming megakaryocytes in the bone marrow. CD41$^+$ megakaryocytes and proplatelet-forming megakaryocytes were both significantly more likely than all CD45$^+$ hematopoietic cells to localize within 10 µm of sinusoids and significantly less likely than all CD45$^+$ cells to localize within 10 µm of arterioles (Figure 3G, 3H and Supplemental Figure 3C). 72±7.5% of megakaryocytes and 93±7.4% of proplatelet-forming megakaryocytes were within 10 µm of sinusoids. CD41$^+$ megakaryocytes and proplatelet-forming megakaryocytes were also significantly more likely than all CD45$^+$ hematopoietic cells to localize within 10 µm of *Cxcl14*-DsRed$^+$ cells: 84±7.8% of megakaryocytes and all proplatelet-forming megakaryocytes were within 10 µm of *Cxcl14*-DsRed$^+$ cells (Figure 3I-J). Lattice light-sheet microscopy revealed that most perisinusoidal megakaryocytes were enveloped by fine processes from *Cxcl14*-DsRed$^+$

stromal cells (Figure 3K-L; see also Video 1). We observed no significant difference in the percentages of megakaryocytes or proplatelet-forming megakaryocytes that localized to sinusoids in *Lepr-cre; Cxcl14*$^{fl/fl}$ versus control mice (Supplemental Figure 3D-E). Therefore, megakaryocytes and proplatelet-forming megakaryocytes localized mainly to sinusoids but CXCL14 did not appear to be necessary for their localization to these perisinusoidal niches.

To test if *Cxcl14* functions locally within individual bone marrow compartments or systematically, we assessed hematopoiesis in the long bones (femurs and tibia) and vertebrae of *Prx1-cre; Cxcl14*$^{fl/fl}$ mice and littermate controls at 6 to 9 months of age. Prx1-cre recombines in limb mesenchyme, including in LepR^{+} cells, but not in vertebrae. Consistent with the phenotype of *Lepr-cre; Cxcl14*$^{fl/fl}$ mice, we observed no significant differences between *Prx1-cre; Cxcl14*$^{fl/fl}$ and littermate control mice in terms of red or white blood cell counts but *Prx1-cre; Cxcl14*$^{fl/fl}$ mice had significantly lower platelet counts (Supplemental Figure 4A). *Prx1-cre; Cxcl14*$^{fl/fl}$ and littermate control mice also did not significantly differ in body mass, bone marrow cellularity, or the frequencies of hematopoietic stem or progenitor cells by flow cytometry in either long bones or vertebrae (Supplemental Figure 4B-AM). However, the number of proplatelet-forming megakaryocytes was significantly lower in femur (Figure 3M), but not vertebra (Figure 3N), bone marrow from *Prx1-cre; Cxcl14*$^{fl/fl}$ as compared to control mice. This suggests that *Cxcl14* acts locally within individual bone marrow compartments to promote platelet formation.

CXCL14 reprograms lipid metabolism in megakaryocytes

We isolated megakaryocytes from the bone marrow of *Lepr-cre; Cxcl14*$^{fl/fl}$ and littermate control mice using paramagnetic beads and performed RNA sequencing. Four of the ten most significantly enriched Gene Ontology (GO) terms among the differentially expressed genes related to megakaryocyte or platelet differentiation (red highlighted gene sets in Figure 4A). Nearly all of the megakaryocyte and platelet differentiation genes[71] detected in our RNA

sequencing were significantly downregulated in megakaryocytes from *Lepr-cre; Cxcl14*$^{fl/fl}$ as compared to control mice (red highlighted genes in Figure 4B).

The molecular function GO term most enriched among the genes that were differentially expressed between *Lepr-cre; Cxcl14*$^{fl/fl}$ and control megakaryocytes related to lipid metabolism (Figure 4C). Scores of genes in this GO term were expressed at significantly lower levels in megakaryocytes from *Lepr-cre; Cxcl14*$^{fl/fl}$ as compared to control mice, including 15 of 17 lipid metabolism genes (Figure 4D). These included *Pparg*, which encodes the PPARγ transcription factor that regulates fatty acid metabolism[72]. PPARγ acts partly by promoting the transcription of fatty acid transporters including *Cd36*, *Fabp5,* and *Fatp4*[73]. The levels of PPARγ, FABP5, FATP4 and CD36 protein were all reduced in CD42d^{+} megakaryocytes isolated using paramagnetic beads from the bone marrow of *Lepr-cre; Cxcl14*$^{fl/fl}$ as compared to control mice (Figure 4E-G). This raised the possibility that megakaryocytes from *Lepr-cre; Cxcl14*$^{fl/fl}$ mice have defects in lipid metabolism, including reduced fatty acid uptake. Changes in lipid metabolism, including increased uptake of polyunsaturated fatty acids, are necessary in megakaryocytes for the formation of proplatelet-forming megakaryocytes and platelets, partly to form the demarcation membrane system[74,75].

We performed lipidomics on CD42d^{+} megakaryocytes isolated using paramagnetic beads from *Lepr-cre; Cxcl14*$^{fl/fl}$ and control bone marrow. We detected 260 lipid species (Supplemental Table 2). All of the lipids that significantly differed between megakaryocytes from *Lepr-cre; Cxcl14*$^{fl/fl}$ and control mice are shown in Figure 4H. Stearic acid was significantly enriched in megakaryocytes from *Lepr-cre; Cxcl14*$^{fl/fl}$ mice while 11 species of triglycerides and 2 species of ceramides were significantly depleted. Most of these triglycerides contained polyunsaturated fatty acids, suggesting depletion of polyunsaturated fatty acids in megakaryocytes from *Lepr-cre; Cxcl14*$^{fl/fl}$ mice. While cells can synthesize their own saturated and monounsaturated fatty acids, polyunsaturated fatty acids must be obtained from the diet[76].

To test if CXCL14 from LepR$^+$ cells promotes polyunsaturated fatty acid uptake by megakaryocytes, we infused *Lepr-cre; Cxcl14$^{fl/fl}$* and littermate control mice for 24 hours with $^{13}C_{18}$-linoleic acid, then isolated CD42d$^+$ megakaryocytes from the bone marrow using paramagnetic beads and assessed the fractional enrichment of ^{13}C-labelled linoleic acid in saponified lipids by mass spectrometry. We observed no significant difference in the fractional enrichment of $^{13}C_{18}$-linoleic acid ($^{13}C_{18}$-linolaic acid/all linoleic acid) in blood plasma from *Lepr-cre; Cxcl14$^{fl/fl}$* and control mice (Figure 4I) but *Lepr-cre; Cxcl14$^{fl/fl}$* megakaryocytes exhibited significantly reduced fractional enrichment as compared to control megakaryocytes (Figure 4J). This suggests that bone marrow megakaryocytes have less capacity to incorporate polyunsaturated fatty acids from circulation in the absence of CXCL14 from LepR$^+$ cells.

A high-fat diet rescued platelet formation in *Lepr-cre; Cxcl14$^{fl/fl}$* mice

If the defects in platelet formation were caused by reduced fatty acid/lipid uptake, we hypothesized these defects would be rescued by feeding the mice a high fat diet. To test this, we fed *Lepr-cre; Cxcl14$^{fl/fl}$* and littermate control mice normal chow (10% of calories from fat) or either of two high fat diets (both with 60% of calories from fat) (see dietary compositions in Figure 5A). High fat diet 1 (HFD1) was particularly enriched for polyunsaturated fatty acids. Both high fat diets significantly increased body mass in *Lepr-cre; Cxcl14$^{fl/fl}$* and control mice as compared to mice fed normal chow (Figure 5B). Neither diet nor mouse genotype significantly altered white blood cell counts (Figure 5C), red blood cell counts (Figure 5D), or bone marrow cellularity (Figure 5F). Platelet counts were significantly reduced in the blood of *Lepr-cre; Cxcl14$^{fl/fl}$* as compared to control mice fed normal chow but did not significantly differ between *Lepr-cre; Cxcl14$^{fl/fl}$* and control mice fed either high fat diet (Figure 5E). This suggested that high fat diets rescued platelet production in *Lepr-cre; Cxcl14$^{fl/fl}$* mice.

Mice on different diets sometimes had statistically significant differences in the frequencies of MPPs and some restricted hematopoietic progenitors; however, *Lepr-cre;*

Cxcl14$^{fl/fl}$ and control mice did not exhibit significant differences in the frequencies of any hematopoietic stem or progenitor cell population in the bone marrow by flow cytometry, irrespective of diet (Supplemental Figure 5A-M). In this experiment, the frequency of CD41^{+}CD42d^{+} megakaryocytes, measured by flow cytometry, was significantly increased in the bone marrow of *Lepr-cre; Cxcl14*$^{fl/fl}$ as compared to control mice fed normal chow but not in mice fed either high fat diet (Supplemental Figure 5N). This may have reflected an effort to compensate for the depletion of platelets in mutant mice.

To assess the effects of high fat diets on mature megakaryocytes, we sectioned the bone marrow of *Lepr-cre; Cxcl14*$^{fl/fl}$ and control mice. Neither diet nor mouse genotype significantly affected the number of CD41^{+} megakaryocytes in bone marrow sections (Figure 5G). The size of these megakaryocytes was significantly reduced in *Lepr-cre; Cxcl14*$^{fl/fl}$ as compared to control mice fed normal chow but no statistically significant difference was observed in mice fed either high fat diet (Figure 5H-I). The number of proplatelet-forming megakaryocytes was significantly reduced in the bone marrow of *Lepr-cre; Cxcl14*$^{fl/fl}$ as compared to control mice fed normal chow but not in mice fed a high fat diet (Figure 5J).

We performed a lipidomic analysis on CD42d^{+} megakaryocytes isolated using paramagnetic beads from the bone marrow of *Lepr-cre; Cxcl14*$^{fl/fl}$ and control mice (see Supplemental Table 3-5 for a list of lipid species detected). The triglycerides that were depleted in *Lepr-cre; Cxcl14*$^{fl/fl}$ megakaryocytes from mice fed normal chow (Supplemental Figure 5O) were not depleted in *Lepr-cre; Cxcl14*$^{fl/fl}$ megakaryocytes from mice fed a high fat diet (Supplemental Figure 5P-Q). Indeed, no lipids were significantly depleted in megakaryocytes from *Lepr-cre; Cxcl14*$^{fl/fl}$ mice fed HFD2 (Supplemental Figure 5Q) and no triglycerides containing polyunsaturated fatty acids were depleted in megakaryocytes from *Lepr-cre; Cxcl14*$^{fl/fl}$ mice fed HFD1 (Supplemental Figure 5P). High fat diet feeding thus eliminated the depletion of triglycerides containing polyunsaturated fatty acids in addition to rescuing the formation of proplatelet-forming megakaryocytes and platelets.

Recombinant CXCL14 is sufficient to promote thrombopoiesis

We cultured CD42d^{+} bone marrow cells with or without recombinant CXCL14 (100 ng/ml). CXCL14 significantly increased the numbers of proplatelet-forming megakaryocytes that formed in culture 16 to 40 hours after adding it (Figure 6B). Since only megakaryocytes were present in these cultures, this observation suggests that CXCL14 acts directly on megakaryocytes to promote their maturation into proplatelet-forming megakaryocytes.

We also intravenously injected wild-type mice with 20 µg/kg recombinant mouse CXCL14 and then analyzed the bone marrow 16 hours later. CXCL14-treated and control mice did not significantly differ in terms of white blood cell or red blood cell counts but the CXCL14-treated mice had significantly higher platelet counts (Figure 6C-E). CXCL14-treated and control mice also did not significantly differ in terms of bone marrow cellularity or the frequencies of HSCs, MPPs, restricted hematopoietic progenitors, or megakaryocytes in the bone marrow by flow cytometry (Figure 6F-T) or in bone marrow sections (Figure 6U-V). However, CXCL14-treated mice had significantly larger megakaryocytes (Figure 6W) and more proplatelet-forming megakaryocytes in the bone marrow as compared to control mice (Figure 6X). Treatment of wild-type mice with CXCL14 was thus sufficient to increase the formation of proplatelet-forming megakaryocytes and platelets.

DISCUSSION

CXCL14 appeared to promote the formation of proplatelet-forming megakaryocytes and platelets by remodeling lipid metabolism in megakaryocytes. Increased polyunsaturated fatty acid uptake is necessary in megakaryocytes to form the demarcation membrane system[74,75]. The triglyceride depletion in the lipidomic analysis of megakaryocytes from *Lepr-cre; Cxcl14*$^{fl/fl}$ mice (Figure 4H) may reflect the consumption of triglycerides in an effort to sustain demarcation membrane synthesis in the absence of CXCL14. A high fat diet rescued the depletion of lipids

and the numbers of proplatelet-forming megakaryocytes and platelets in *Lepr-cre; Cxcl14*$^{fl/fl}$ mice (Figure 5E-M). To our knowledge, these data provide the first evidence that LepR^{+} cells regulate metabolism and terminal differentiation in some hematopoietic cells, broadening the scope of mechanisms by which LepR^{+} cells regulate hematopoiesis.

The fatty acid transporters whose expression declined in megakaryocytes from *Lepr-cre; Cxcl14*$^{fl/fl}$ mice as compared to littermate controls (CD36, FATP4, and FABP5) are not specific for polyunsaturated fatty acids[77]. Yet polyunsaturated fatty acid-containing lipids were most prominently depleted from these megakaryocytes (Figure 4H). Cells can synthesize their own saturated and monounsaturated fatty acids, but not polyunsaturated fatty acids, potentially compensating for the reduced uptake of saturated and monounsaturated fatty acids[76,78]. It is also possible that the depletion of polyunsaturated fatty acid-containing triglycerides in megakaryocytes from *Lepr-cre; Cxcl14*$^{fl/fl}$ mice reflects broader defects in lipid uptake or lipid metabolism, not just reduced expression of fatty acid transporters. In future studies, it will be interesting to better understand the mechanisms by which CXCL14 regulates lipid metabolism in megakaryocytes, including identifying the receptor for CXCL14 on megakaryocytes.

ACKNOWLEDGEMENTS

S.J.M. is a Howard Hughes Medical Institute (HHMI) Investigator, the Mary McDermott Cook Chair in Pediatric Genetics, the Kathryn and Gene Bishop Distinguished Chair in Pediatric Research, the director of the Hamon Laboratory for Stem Cells and Cancer, and a Cancer Prevention and Research Institute of Texas Scholar. This study was supported partly by funding from the National Institutes of Health (DK118745 to S.J.M.) and the Moody Medical Research Institute (to S.J.M.). R.J.D. is an HHMI Investigator and is supported by NIH grant R35CA220449. DL is a scholar of Blood Cancer United. TPM and the CRI Metabolomics Facility are supported by funding from the Cancer Prevention Research Institute of Texas (CPRIT Core Facilities Support Award RP240494). We thank the BioHPC high performance computing cloud

at UT Southwestern Medical Center for providing computational resources and the Moody Foundation Flow Cytometry Facility. We thank the electron microscopy core facility, supported by NIH grant 1S10OD021685. This article is subject to HHMI's Open Access to Publications policy. HHMI lab heads have previously granted a nonexclusive CC BY 4.0 license to the public and a sublicensable license to HHMI in their research articles. Pursuant to those licenses, the author-accepted manuscript of this article can be made freely available under a CC BY 4.0 license immediately upon publication.

AUTHOR CONTRIBUTIONS

Y.X. and S.J.M. conceived the project and designed and interpreted experiments. Y.X. performed most of the experiments, with general technical assistance from A.R. and R.Z. and advice and technical assistance in the lipidomic analysis experiments from S.M. and G.G.. M.L. performed the western blots and T.T. implanted jugular catheters in mice for isotope-labelled linoleic acid infusion. T.M., Y.L., W.G., and R.D. helped to perform and analyze the isotope tracing experiments. T.N., Z.S., E.J., and K.D. provided the light-sheet microscopy platform, performed the imaging, and analyzed the light-sheet imaging data. N.J., T.W., and L.D. helped to prepare samples and perform flow cytometry in experiments that involved many mice. Y.Z. and D.L. originally observed the fine processes from $LepR^+$ cells that envelop megakaryocytes and suggested we test if this was true of CXCL14-expressing cells. Z.Z. performed statistical analyses. Y.X. and S.J.M. wrote the manuscript.

CONFLICT OF INTEREST DISCLOSURE

The authors declare no competing interests.

REFERENCES

1. Ding L, Saunders TL, Enikolopov G, Morrison SJ. Endothelial and perivascular cells maintain haematopoietic stem cells. *Nature*. 2012;481(7382):457-462.
2. Comazzetto S, Murphy MM, Berto S, Jeffery E, Zhao Z, Morrison SJ. Restricted Hematopoietic Progenitors and Erythropoiesis Require SCF from Leptin Receptor+ Niche Cells in the Bone Marrow. *Cell Stem Cell*. 2019;24(3):477-486 e476.
3. Oguro H, Ding L, Morrison SJ. SLAM family markers resolve functionally distinct subpopulations of hematopoietic stem cells and multipotent progenitors. *Cell Stem Cell*. 2013;13(1):102-116.
4. Ding L, Morrison SJ. Haematopoietic stem cells and early lymphoid progenitors occupy distinct bone marrow niches. *Nature*. 2013;495(7440):231-235.
5. Greenbaum A, Hsu YM, Day RB, et al. CXCL12 in early mesenchymal progenitors is required for haematopoietic stem-cell maintenance. *Nature*. 2013;495(7440):227-230.
6. Himburg HA, Termini CM, Schlussel L, et al. Distinct Bone Marrow Sources of Pleiotrophin Control Hematopoietic Stem Cell Maintenance and Regeneration. *Cell Stem Cell*. 2018;23(3):370-381 e375.
7. Cordeiro Gomes A, Hara T, Lim VY, et al. Hematopoietic Stem Cell Niches Produce Lineage-Instructive Signals to Control Multipotent Progenitor Differentiation. *Immunity*. 2016;45(6):1219-1231.
8. Emoto T, Lu J, Sivasubramaniyam T, et al. Colony stimulating factor-1 producing endothelial cells and mesenchymal stromal cells maintain monocytes within a perivascular bone marrow niche. *Immunity*. 2022;55(5):862-878 e868.
9. Zhong L, Lu J, Fang J, et al. Csf1 from marrow adipogenic precursors is required for osteoclast formation and hematopoiesis in bone. *Elife*. 2023;12.
10. Inoue K, Qin Y, Xia Y, et al. Bone marrow Adipoq-lineage progenitors are a major cellular source of M-CSF that dominates bone marrow macrophage development, osteoclastogenesis, and bone mass. *Elife*. 2023;12.
11. Omatsu Y, Sugiyama T, Kohara H, et al. The essential functions of adipo-osteogenic progenitors as the hematopoietic stem and progenitor cell niche. *Immunity*. 2010;33(3):387-399.
12. Sugiyama T, Kohara H, Noda M, Nagasawa T. Maintenance of the hematopoietic stem cell pool by CXCL12-CXCR4 chemokine signaling in bone marrow stromal cell niches. *Immunity*. 2006;25(6):977-988.
13. Zhang J, Wu Q, Johnson CB, et al. In situ mapping identifies distinct vascular niches for myelopoiesis. *Nature*. 2021;590(7846):457-462.
14. Wu Q, Zhang J, Kumar S, et al. Resilient anatomy and local plasticity of naive and stress haematopoiesis. *Nature*. 2024;627(8005):839-846.
15. Acar M, Kocherlakota KS, Murphy MM, et al. Deep imaging of bone marrow shows non-dividing stem cells are mainly perisinusoidal. *Nature*. 2015;526(7571):126-130.
16. Shen B, Tasdogan A, Ubellacker JM, et al. A mechanosensitive peri-arteriolar niche for osteogenesis and lymphopoiesis. *Nature*. 2021;591(7850):438-444.
17. Zhou BO, Ding L, Morrison SJ. Hematopoietic stem and progenitor cells regulate the regeneration of their niche by secreting Angiopoietin-1. *Elife*. 2015;4:e05521.
18. Fang S, Chen S, Nurmi H, et al. VEGF-C protects the integrity of the bone marrow perivascular niche in mice. *Blood*. 2020;136(16):1871-1883.
19. Gao X, Murphy MM, Peyer JG, et al. Leptin receptor(+) cells promote bone marrow innervation and regeneration by synthesizing nerve growth factor. *Nat Cell Biol*. 2023;25(12):1746-1757.
20. Gawaz M, Vogel S. Platelets in tissue repair: control of apoptosis and interactions with regenerative cells. *Blood*. 2013;122(15):2550-2554.

21. Asquith NL, Carminita E, Camacho V, et al. The bone marrow is the primary site of thrombopoiesis. *Blood*. 2024;143(3):272-278.
22. Machlus KR, Italiano JE, Jr. The incredible journey: From megakaryocyte development to platelet formation. *J Cell Biol*. 2013;201(6):785-796.
23. Stegner D, vanEeuwijk JMM, Angay O, et al. Thrombopoiesis is spatially regulated by the bone marrow vasculature. *Nat Commun*. 2017;8(1):127.
24. Avecilla ST, Hattori K, Heissig B, et al. Chemokine-mediated interaction of hematopoietic progenitors with the bone marrow vascular niche is required for thrombopoiesis. *Nat Med*. 2004;10(1):64-71.
25. Junt T, Schulze H, Chen Z, et al. Dynamic visualization of thrombopoiesis within bone marrow. *Science*. 2007;317(5845):1767-1770.
26. Kaushansky K, Lok S, Holly RD, et al. Promotion of megakaryocyte progenitor expansion and differentiation by the c-Mpl ligand thrombopoietin. *Nature*. 1994;369(6481):568-571.
27. de Sauvage FJ, Hass PE, Spencer SD, et al. Stimulation of megakaryocytopoiesis and thrombopoiesis by the c-Mpl ligand. *Nature*. 1994;369(6481):533-538.
28. Wendling F, Maraskovsky E, Debili N, et al. cMpl ligand is a humoral regulator of megakaryocytopoiesis. *Nature*. 1994;369(6481):571-574.
29. Debili N, Masse JM, Katz A, Guichard J, Breton-Gorius J, Vainchenker W. Effects of the recombinant hematopoietic growth factors interleukin-3, interleukin-6, stem cell factor, and leukemia inhibitory factor on the megakaryocytic differentiation of CD34+ cells. *Blood*. 1993;82(1):84-95.
30. Briddell RA, Bruno E, Cooper RJ, Brandt JE, Hoffman R. Effect of c-kit ligand on in vitro human megakaryocytopoiesis. *Blood*. 1991;78(11):2854-2859.
31. Avraham H, Vannier E, Cowley S, et al. Effects of the stem cell factor, c-kit ligand, on human megakaryocytic cells. *Blood*. 1992;79(2):365-371.
32. Metcalf D, Hilton D, Nicola NA. Leukemia inhibitory factor can potentiate murine megakaryocyte production in vitro. *Blood*. 1991;77(10):2150-2153.
33. Sakamoto H, Ochiya T, Sato Y, et al. Adenovirus-mediated transfer of the HST-1 (FGF4) gene induces increased levels of platelet count in vivo. *Proc Natl Acad Sci U S A*. 1994;91(26):12368-12372.
34. Konishi H, Ochiya T, Sakamoto H, et al. Effective prevention of thrombocytopenia in mice using adenovirus-mediated transfer of HST-1 (FGF-4) gene. *J Clin Invest*. 1995;96(2):1125-1130.
35. Bruno E, Briddell RA, Cooper RJ, Hoffman R. Effects of recombinant interleukin 11 on human megakaryocyte progenitor cells. *Exp Hematol*. 1991;19(5):378-381.
36. Ishibashi T, Burstein SA. Interleukin 3 promotes the differentiation of isolated single megakaryocytes. *Blood*. 1986;67(5):1512-1514.
37. Ishibashi T, Kimura H, Uchida T, Kariyone S, Friese P, Burstein SA. Human interleukin 6 is a direct promoter of maturation of megakaryocytes in vitro. *Proc Natl Acad Sci U S A*. 1989;86(15):5953-5957.
38. Teramura M, Kobayashi S, Hoshino S, Oshimi K, Mizoguchi H. Interleukin-11 enhances human megakaryocytopoiesis in vitro. *Blood*. 1992;79(2):327-331.
39. Decker M, Leslie J, Liu Q, Ding L. Hepatic thrombopoietin is required for bone marrow hematopoietic stem cell maintenance. *Science*. 2018;360(6384):106-110.
40. Wang JF, Liu ZY, Groopman JE. The alpha-chemokine receptor CXCR4 is expressed on the megakaryocytic lineage from progenitor to platelets and modulates migration and adhesion. *Blood*. 1998;92(3):756-764.
41. Hamada T, Mohle R, Hesselgesser J, et al. Transendothelial migration of megakaryocytes in response to stromal cell-derived factor 1 (SDF-1) enhances platelet formation. *J Exp Med*. 1998;188(3):539-548.

42. Li JJ, Liu J, Li YE, et al. Differentiation route determines the functional outputs of adult megakaryopoiesis. *Immunity*. 2024;57(3):478-494 e476.
43. Rodriguez-Fraticelli AE, Wolock SL, Weinreb CS, et al. Clonal analysis of lineage fate in native haematopoiesis. *Nature*. 2018;553(7687):212-216.
44. Notta F, Zandi S, Takayama N, et al. Distinct routes of lineage development reshape the human blood hierarchy across ontogeny. *Science*. 2016;351(6269):aab2116.
45. Yamamoto R, Morita Y, Ooehara J, et al. Clonal analysis unveils self-renewing lineage-restricted progenitors generated directly from hematopoietic stem cells. *Cell*. 2013;154(5):1112-1126.
46. Carrelha J, Meng Y, Kettyle LM, et al. Hierarchically related lineage-restricted fates of multipotent haematopoietic stem cells. *Nature*. 2018;554(7690):106-111.
47. Poscablo DM, Worthington AK, Smith-Berdan S, et al. An age-progressive platelet differentiation path from hematopoietic stem cells causes exacerbated thrombosis. *Cell*. 2024;187(12):3090-3107 e3021.
48. Chen S, Hu M, Shen M, et al. IGF-1 facilitates thrombopoiesis primarily through Akt activation. *Blood*. 2018;132(2):210-222.
49. Nishimura S, Nagasaki M, Kunishima S, et al. IL-1alpha induces thrombopoiesis through megakaryocyte rupture in response to acute platelet needs. *J Cell Biol*. 2015;209(3):453-466.
50. Machlus KR, Johnson KE, Kulenthirarajan R, et al. CCL5 derived from platelets increases megakaryocyte proplatelet formation. *Blood*. 2016;127(7):921-926.
51. Gaertner F, Ishikawa-Ankerhold H, Stutte S, et al. Plasmacytoid dendritic cells control homeostasis of megakaryopoiesis. *Nature*. 2024;631(8021):645-653.
52. Hromas R, Broxmeyer HE, Kim C, et al. Cloning of BRAK, a novel divergent CXC chemokine preferentially expressed in normal versus malignant cells. *Biochem Biophys Res Commun*. 1999;255(3):703-706.
53. Dolinska M, Cai H, Mansson A, et al. Characterization of the bone marrow niche in patients with chronic myeloid leukemia identifies CXCL14 as a new therapeutic option. *Blood*. 2023;142(1):73-89.
54. Witte A, Rohlfing AK, Dannenmann B, et al. The chemokine CXCL14 mediates platelet function and migration via direct interaction with CXCR4. *Cardiovasc Res*. 2021;117(3):903-917.
55. Tanegashima K, Suzuki K, Nakayama Y, et al. CXCL14 is a natural inhibitor of the CXCL12-CXCR4 signaling axis. *FEBS Lett*. 2013;587(12):1731-1735.
56. Cheng CL, Yang SC, Lai CY, et al. CXCL14 Maintains hESC Self-Renewal through Binding to IGF-1R and Activation of the IGF-1R Pathway. *Cells*. 2020;9(7).
57. Wang Y, Weng X, Wang L, et al. HIC1 deletion promotes breast cancer progression by activating tumor cell/fibroblast crosstalk. *J Clin Invest*. 2018;128(12):5235-5250.
58. Wang X, Menezes CJ, Jia Y, et al. Metabolic inflexibility promotes mitochondrial health during liver regeneration. *Science*. 2024;384(6701):eadj4301.
59. Miyajima R, Tanegashima K, Naruse N, Denda M, Hara T, Otaka A. Identification of Low-Density Lipoprotein Receptor-Related Protein 1 as a CXCL14 Receptor Using Chemically Synthesized Tetrafunctional Probes. *ACS Chem Biol*. 2024;19(2):551-562.
60. Salogni L, Musso T, Bosisio D, et al. Activin A induces dendritic cell migration through the polarized release of CXC chemokine ligands 12 and 14. *Blood*. 2009;113(23):5848-5856.
61. Lu J, Chatterjee M, Schmid H, Beck S, Gawaz M. CXCL14 as an emerging immune and inflammatory modulator. *J Inflamm (Lond)*. 2016;13:1.
62. DeFalco J, Tomishima M, Liu H, et al. Virus-assisted mapping of neural inputs to a feeding center in the hypothalamus. *Science*. 2001;291(5513):2608-2613.
63. Logan M, Martin JF, Nagy A, Lobe C, Olson EN, Tabin CJ. Expression of Cre Recombinase in the developing mouse limb bud driven by a Prxl enhancer. *Genesis*. 2002;33(2):77-80.

64. Ubellacker JM, Tasdogan A, Ramesh V, et al. Lymph protects metastasizing melanoma cells from ferroptosis. *Nature*. 2020;585(7823):113-118.
65. Abbas-Aghababazadeh F, Li Q, Fridley BL. Comparison of normalization approaches for gene expression studies completed with high-throughput sequencing. *PLoS One*. 2018;13(10):e0206312.
66. DeVilbiss AW, Zhao Z, Martin-Sandoval MS, et al. Metabolomic profiling of rare cell populations isolated by flow cytometry from tissues. *Elife*. 2021;10.
67. Faubert B, Tasdogan A, Morrison SJ, Mathews TP, DeBerardinis RJ. Stable isotope tracing to assess tumor metabolism in vivo. *Nat Protoc*. 2021;16(11):5123-5145.
68. Kara N, Xue Y, Zhao Z, et al. Endothelial and Leptin Receptor(+) cells promote the maintenance of stem cells and hematopoiesis in early postnatal murine bone marrow. *Dev Cell*. 2023;58(5):348-360 e346.
69. Mazzi S, Lordier L, Debili N, Raslova H, Vainchenker W. Megakaryocyte and polyploidization. *Exp Hematol*. 2018;57:1-13.
70. Eckly A, Heijnen H, Pertuy F, et al. Biogenesis of the demarcation membrane system (DMS) in megakaryocytes. *Blood*. 2014;123(6):921-930.
71. Haas S, Hansson J, Klimmeck D, et al. Inflammation-Induced Emergency Megakaryopoiesis Driven by Hematopoietic Stem Cell-like Megakaryocyte Progenitors. *Cell Stem Cell*. 2015;17(4):422-434.
72. Ahmadian M, Suh JM, Hah N, et al. PPARgamma signaling and metabolism: the good, the bad and the future. *Nat Med*. 2013;19(5):557-566.
73. Goto K, Iso T, Hanaoka H, et al. Peroxisome proliferator-activated receptor-gamma in capillary endothelia promotes fatty acid uptake by heart during long-term fasting. *J Am Heart Assoc*. 2013;2(1):e004861.
74. de Jonckheere B, Kollotzek F, Munzer P, et al. Critical shifts in lipid metabolism promote megakaryocyte differentiation and proplatelet formation. *Nat Cardiovasc Res*. 2023;2:835-852.
75. Barrachina MN, Pernes G, Becker IC, et al. Efficient megakaryopoiesis and platelet production require phospholipid remodeling and PUFA uptake through CD36. *Nat Cardiovasc Res*. 2023;2(8):746-763.
76. Jeon YG, Kim YY, Lee G, Kim JB. Physiological and pathological roles of lipogenesis. *Nat Metab*. 2023;5(5):735-759.
77. Stahl A, Gimeno RE, Tartaglia LA, Lodish HF. Fatty acid transport proteins: a current view of a growing family. *Trends Endocrinol Metab*. 2001;12(6):266-273.
78. Rohrig F, Schulze A. The multifaceted roles of fatty acid synthesis in cancer. *Nat Rev Cancer*. 2016;16(11):732-749.

FIGURE LEGENDS

Figure 1: LepR$^+$ stromal cells were the main source of *Cxcl14* in the bone marrow. (A) Single cell RNA sequencing[68] showing *Cxcl14* expression by LepR$^+$ stromal cells from enzymatically dissociated bone and bone marrow (a total of 3-4 mice from 3 independent experiments). (B) *Cxcl14* expression by quantitative reverse-transcription PCR in CD150$^+$CD48$^-$ Lineage$^-$Sca1$^+$ckit$^+$ HSCs, CD31$^+$CD45$^-$Ter119$^-$ endothelial cells, LepR$^+$CD45$^-$Ter119$^-$CD31$^-$ stromal cells, and unfractionated cells from the bone marrow of two month-old mice (a total of 3 samples per cell population from 3 independent experiments; each dot represents a different sample). (C and D) Deep confocal imaging of femur bone marrow from adult *Cxcl14*^{dsRed}*Scf*^{GFP} mice: *Cxcl14*-dsRed$^+$ cells localized around sinusoids (arrowheads) and arterioles (arrow) throughout bone marrow. Most *Cxcl14*-dsRed$^+$ cells were *Scf*-GFP$^+$ (images are representative of 3 mice). (E) Femur bone marrow from adult *Cxcl14*^{dsRed} mice stained with anti-LepR antibody showing that most *Cxcl14*-dsRed$^+$ cells were LepR$^+$ (images are representative of 3 mice). (F-J) Flow cytometric analysis of enzymatically dissociated bone marrow from *Cxcl14*$^{dsRed/+}$ or *Cxcl14*^{dsRed}*Scf*^{GFP} mice. Only 0.19±0.04% of bone marrow cells from *Cxcl14*$^{dsRed/+}$ mice were *Cxcl14*-dsRed$^+$ and, of these, 91% were LepR$^+$ (F). Conversely, 89% of LepR$^+$ cells were *Cxcl14*-dsRed$^+$ (G). 84% of LepR$^+$ cells from bone marrow of *Cxcl14*^{dsRed}*Scf*^{GFP} mice were *Cxcl14*-dsRed$^+$ and *Scf*-GFP$^+$ (H). Few CD31$^+$CD45$^-$Ter119$^-$ endothelial cells from bone marrow of *Cxcl14*$^{dsRed/+}$ mice were *Cxcl14*-dsRed$^+$ (I; 3-6 mice from 3 independent experiments). (J) Flow cytometric analysis of non-enzymatically dissociated bone marrow shows few or no CD45$^+$ cells expressed *Cxcl14*-dsRed (3-6 mice from 3 independent experiments; see also Supplemental Figure1D). Data represent mean ± standard deviation in panels B, F, G, and I.

Figure 2: *Lepr-cre; Cxcl14*$^{fl/fl}$ mice exhibited grossly normal hematopoiesis but reduced platelet counts. (A-U) Bone marrow cellularity (A) and the frequencies of HSCs (B), MPPs (C), HPCs (D), CMPs (E), GMPs (F), MEPs (G), CLPs (H), Pre-GMs (I), Pre-CFUEs (J), CFU-Es

(K), Pre-MegEs (L), megakaryocyte progenitors (M), Pre-proB cells (N), ProB cells (O), PreB cells (P), Myeloid cells (Q), B220^{+}IgM^{+} B cells (R), CD3^{+} T cells (S) CD41^{+}CD42d^{-} megakaryocytes (T) and CD41^{+}CD42d^{+} megakaryocytes (U) in the bone marrow of *Lepr-cre; Cxcl14* $^{fl/fl}$ and littermate control mice at 4 months of age (a total of 4-17 mice per genotype from 3-7 independent experiments; each dot represents a different mouse in panels A-X). (V) White blood cell (WBC), red blood cell (RBC) and platelet (PLT) counts in the blood of *Lepr-cre; Cxcl14*$^{fl/fl}$ mice and littermate controls at 4 months of age (V; a total of 6-17 mice per genotype from 7 independent experiments) and 7 months of age (W; a total of 4-5 mice per genotype from 3 independent experiments). (X) Bleeding time after severing the tail 1 mm from the end in *Lepr-cre; Cxcl14*$^{fl/fl}$ and control mice (a total of 14-15 mice per genotype from 3 independent experiments). (Y) WBC, RBC and PLT counts from the blood of *Lepr-cre; Cxcl14*$^{fl/fl}$ and control mice before (day 0) and 2, 4, 6 and 12 days after treatment with anti-CD42b antibody to deplete platelets (a total of 6 mice per genotype from 2 independent experiments). (Z) WBC, RBC and PLT counts from *Lepr-cre; Cxcl14*$^{fl/fl}$ and control mice before (day 0) and 7, 14, 28 and 35 days after sublethal irradiation (a total of 4-8 mice per genotype from 2 independent experiments). All data represent mean ± standard deviation. All statistical tests were two-sided. Statistical significance was assessed using Student's *t*-tests (A and X), Mann-Whitney tests followed by Holm-Sidak's multiple comparisons adjustments (B-U), or Student's *t*-tests followed by Holm-Sidak's multiple comparisons adjustments (V, W, Y and Z).

Figure 3: *Lepr-cre; Cxcl14*$^{fl/fl}$ mice produced fewer proplatelet-forming megakaryocytes in the bone marrow. (A) Representative images of femur bone marrow from adult *Lepr-cre; Cxcl14*$^{fl/fl}$ and control mice showing CD41^{+} megakaryocytes (arrows point to proplatelet-forming megakaryocytes; image is representative of 3 independent experiments). (B) The number of CD41^{+} megakaryocytes per mm^{2} in bone marrow sections did not significantly differ between

Lepr-cre; Cxcl14$^{fl/fl}$ and control mice (3 mice per genotype from 3 independent experiments). (C) Distribution of CD41^{+} megakaryocyte cell diameters (3 mice per genotype from 3 independent experiments). (D) The number of CD41^{+} proplatelet-forming megakaryocytes (PPF MKs) per mm^{2} in bone marrow sections (3 mice per genotype from 3 independent experiments). (E, F) Transmission microscopy images of megakaryocytes in the bone marrow of *Lepr-cre; Cxcl14*$^{fl/fl}$ and control mice showed reduced demarcation membrane system (DMS) in megakaryocytes from mutant mice (3 mice per genotype from 3 independent experiments; each dot represents a megakaryocyte). (G, H) CD41^{+} megakaryocytes (G) and CD41^{+} proplatelet-forming megakaryocytes (H) were significantly more likely than all CD45^{+} cells to localize adjacent to sinusoids and less likely to localize adjacent to arterioles (a total of 3 mice per group from 3 independent experiments). (I, J) CD41^{+} megakaryocytes (I) and CD41^{+} proplatelet-forming megakaryocytes (J) were significantly more likely than all CD45^{+} cells to localize adjacent to *Cxcl14*-dsRed^{+} stromal cells (3 or 5 mice per group from 3 independent experiments). (K-L) Representative images of femur bone marrow from *Cxcl14*^{dsRed} mice showing fine processes from *Cxcl14*$^{+}$ stromal cells wrapping around CD41^{+} megakaryocytes (images are representative of 4 independent experiments). (M, N) The number of CD41^{+} proplatelet-forming megakaryocytes (PPF MKs) per mm^{2} of bone marrow sections from femurs (M) or vertebrae (N) of *Prx1-cre; Cxcl14*$^{fl/fl}$ and control mice (6 or 9 mice per genotype from 3 or 4 independent experiments). All data represent mean ± standard deviation and each dot represents a different mouse except in panels C and F. All statistical tests were two-sided. Statistical significance was assessed using matched samples two-way ANOVAs followed by Sidak's multiple comparisons adjustments (B and D), nested *t*-tests (C and F), Student's *t*-tests (G, H, I, J, and M) , or Mann-Whitney tests (J, and N) followed by Holm-Sidak's multiple comparisons adjustments.

Figure 4: Megakaryocytes from *Lepr-cre; Cxcl14$^{fl/fl}$* mice exhibited changes in lipid metabolism as compared to control megakaryocytes. (A-D) We performed RNA sequencing on megakaryocytes from the bone marrow of *Lepr-cre; Cxcl14$^{fl/fl}$* and control mice (3 mice per genotype from 3 independent experiments). (A) The 10 most significant Gene Ontology (GO) terms that were enriched for genes differentially expressed among *Lepr-cre; Cxcl14$^{fl/fl}$* and control megakaryocytes (log2 fold change > 0.5 in either direction and FDR < 0.05), including GO terms related to biological processes (BP), cellular components (CC) and molecular function (MF). GO terms highlighted in red contain genes involved in megakaryocyte and platelet differentiation or function. (B) Heatmap of genes involved in megakaryocyte or platelet differentiation (z scores; list of genes is from ref[71]). (C) The 10 most significantly enriched GO terms related to molecular function (MF) from genes that were differentially expressed among *Lepr-cre; Cxcl14$^{fl/fl}$* and control megakaryocytes (log2 fold change >0.5 in either direction and FDR < 0.05). (D) Heatmap of genes from the lipid binding GO term that were directly related to lipid metabolism (z scores). (E-G) Western blot of proteins that regulate lipid metabolism or fatty acid transport in extracts from CD42d^{+} megakaryocytes isolated using paramagnetic beads from *Lepr-cre; Cxcl14$^{fl/fl}$* or littermate control bone marrow (results are representative of 2 samples per genotype from 2 independent experiments). (H) Lipidomic analysis of CD42d^{+} megakaryocytes from *Lepr-cre; Cxcl14$^{fl/fl}$* and control bone marrow. Significantly changed lipid species (FDR<0.05, log2 FC>0.5 in either direction) in megakaryocytes from *Lepr-cre; Cxcl14$^{fl/fl}$* as compared to control bone marrow. (I and J) Fractional enrichment of $^{13}C_{18}$-linoleic acid in blood plasma or megakaryocytes from *Lepr-cre; Cxcl14$^{fl/fl}$* and control mice after intravenous infusion of $^{13}C_{18}$-linoleic acid for 24 hours (a total of 7 mice per genotype from 2 independent experiments). All statistical tests were two-sided. Statistical significance was assessed using the Omics Data Analyzer (see lipidomics methods; H), a Mann-Whitney test (I) and a Student's *t*-test (J) followed by Holm-Sidak's multiple comparisons adjustments.

Figure 5: High-fat diet feeding rescued thrombopoiesis in *Lepr-cre; Cxcl14$^{fl/fl}$* mice. (A-M) *Lepr-cre; Cxcl14$^{fl/fl}$* and littermate control mice were fed normal chow (10% of calories from fat) or either of two high fat diets (HFD1 and HFD2, both of which had 60% of calories from fat) for four weeks. (B) Body mass of *Lepr-cre; Cxcl14$^{fl/fl}$* and control mice after 4 weeks on these diets (a total of 3-13 mice per genotype per diet from 2-3 independent experiments). (C-F) Blood cell counts and bone marrow cellularity (F) in *Lepr-cre; Cxcl14$^{fl/fl}$* and control mice fed each diet (a total of 3-16 mice per genotype per diet from 2-3 independent experiments; each dot represents a different mouse). (G-I) The number of CD41^{+} megakaryocytes per mm^{2} in sections through the bone marrow (G) and the cell diameter distribution of these cells in mice fed normal chow versus HFD1 (H) or normal chow versus HFD2 (I). (J) The number of CD41^{+} proplatelet-forming megakaryocytes per mm^{2} in sections through the bone marrow of mice on control, HFD1, or HFD2 diets (3 mice per genotype from 3 independent experiments in G-J). All data represent mean ± standard deviation and each dot represents a different mouse except in panels H and I. All statistical tests were two-sided. Statistical significance was assessed using two-way ANOVAs followed by Sidak's or Dunnett's multiple comparisons adjustments (B, F, G, and J), Mann-Whitney tests followed by Holm-Sidak's multiple comparisons adjustments (C-E), a nested one-way ANOVAs followed by Sidak's multiple comparisons adjustments (H and I).

Figure 6: Recombinant CXCL14 is sufficient to increase the production of proplatelet-forming megakaryocytes and platelets. (A, B) Proplatelet-forming megakaryocytes (arrows) formed by CD42^{+} bone marrow cells cultured with or without 100 ng/mL recombinant mouse CXCL14 (rmCXCL14) (images are representative of 5 independent experiments). (C-X) Wild-type mice were intravenously injected with recombinant mouse CXCL14 and then analyzed 16 hours later. Panels C-T show 6 mice per treatment from 3 independent experiments. (C-E)

Blood cell counts. (F-T) Bone marrow cellularity (F) and the frequencies of HSCs (G), MPPs (H), HPCs (I), CLPs (J), CMPs (K), GMPs (L), MEPs (M), Pre-GMs (N), Pre-CFU-Es (O), CFU-Es (P), Pre-MegEs (Q), megakaryocyte progenitors (R), $CD41^{+}CD42d^{-}$ megakaryocytes (S) and $CD41^{+}CD42d^{+}$ megakaryocytes (T) in the bone marrow. (U) $CD41^{+}$ megakaryocytes in femur diaphysis bone marrow (arrows point to proplatelet-forming megakaryocytes; images are representative of 4 mice per treatment from 3 independent experiments). (V and W) Number of $CD41^{+}$ megakaryocytes per mm^2 in diaphysis bone marrow sections (V) as well as cell diameter distribution (W) (4 mice per group from 3 independent experiments). (X) Number of $CD41^{+}$ proplatelet-forming megakaryocytes per mm^2 in diaphysis bone marrow sections (4 mice per treatment from 3 independent experiments). All data represent mean ± standard deviation and each dot represents a different mouse except in panels B and W. All statistical tests were two-sided. Statistical significance was assessed using Student's *t*-tests followed by Holm-Sidak's multiple comparisons adjustments (C-E), a Student's *t*-test (F), matched samples two-way ANOVAs followed by Sidak's multiple comparisons adjustments (B, G-T, V, and X), or a nested *t*-test (W).

Figure 1

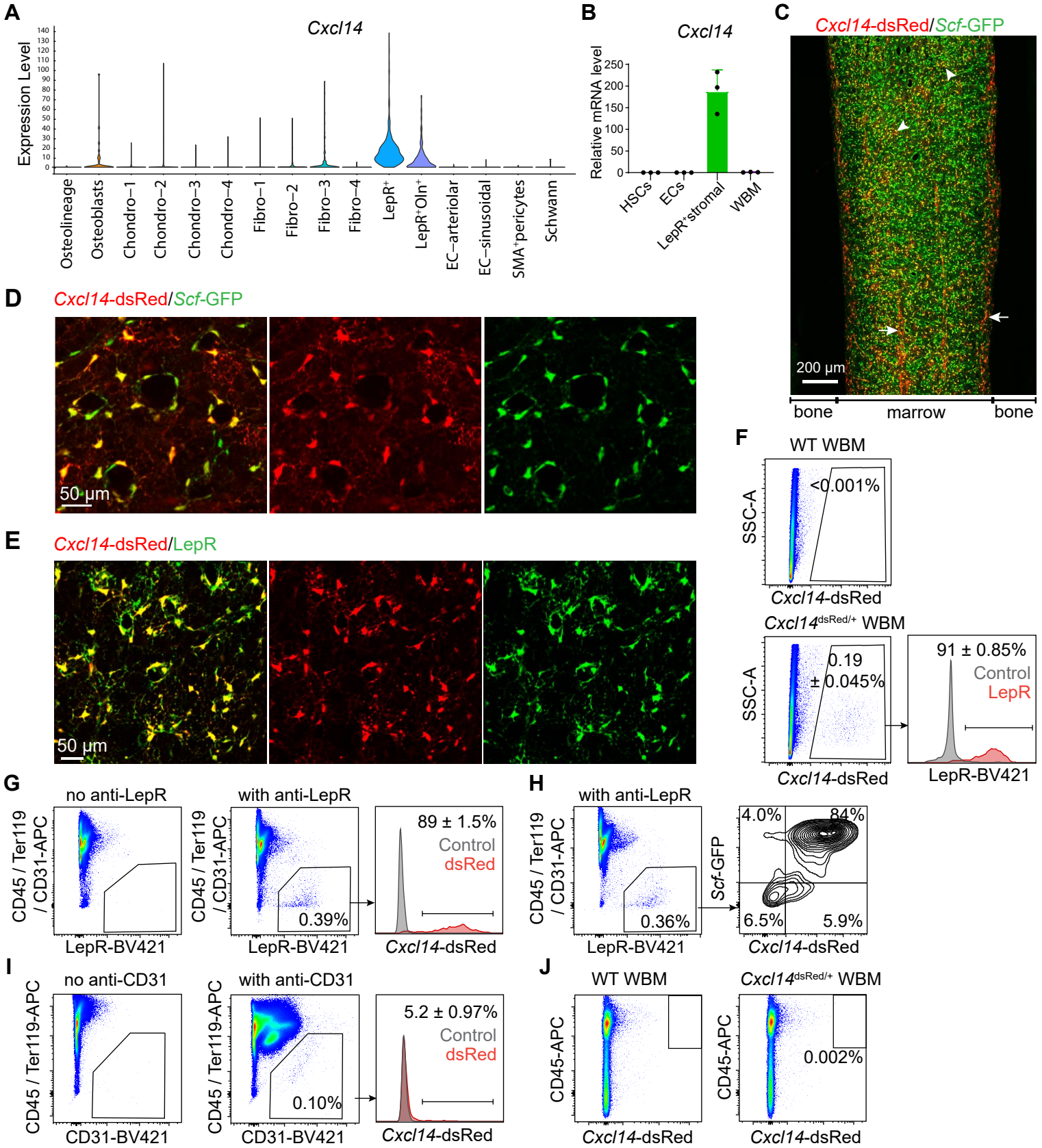
A
Cxcl14
Expression Level
Osteolineage
Osteoblasts
Chondro−1
Chondro−2
Chondro−3
Chondro−4
Fibro−1
Fibro−2
Fibro−3
Fibro−4
LepR+
LepR+Oln+
EC−arteriolar
EC−sinusoidal
SMA+pericytes
Schwann
B
Cxcl14
Relative mRNA level
HSCs
ECs
LepR+stromal
WBM
C
Cxcl14-dsRed/Scf-GFP
200 µm
bone
marrow
bone
D
Cxcl14-dsRed/Scf-GFP
50 µm
E
Cxcl14-dsRed/LepR
50 µm
F
WT WBM
<0.001%
SSC-A
Cxcl14-dsRed
Cxcl14dsRed/+ WBM
0.19
± 0.045%
91 ± 0.85%
Control
LepR
LepR-BV421
G
no anti-LepR
with anti-LepR
CD45 / Ter119 / CD31-APC
LepR-BV421
0.39%
89 ± 1.5%
Control
dsRed
Cxcl14-dsRed
H
with anti-LepR
0.36%
Scf-GFP
4.0%
84%
6.5%
5.9%
I
no anti-CD31
with anti-CD31
CD45 / Ter119-APC
CD31-BV421
0.10%
5.2 ± 0.97%
Control
dsRed
Cxcl14-dsRed
J
WT WBM
Cxcl14dsRed/+ WBM
CD45-APC
0.002%
Cxcl14-dsRed

Figure 2

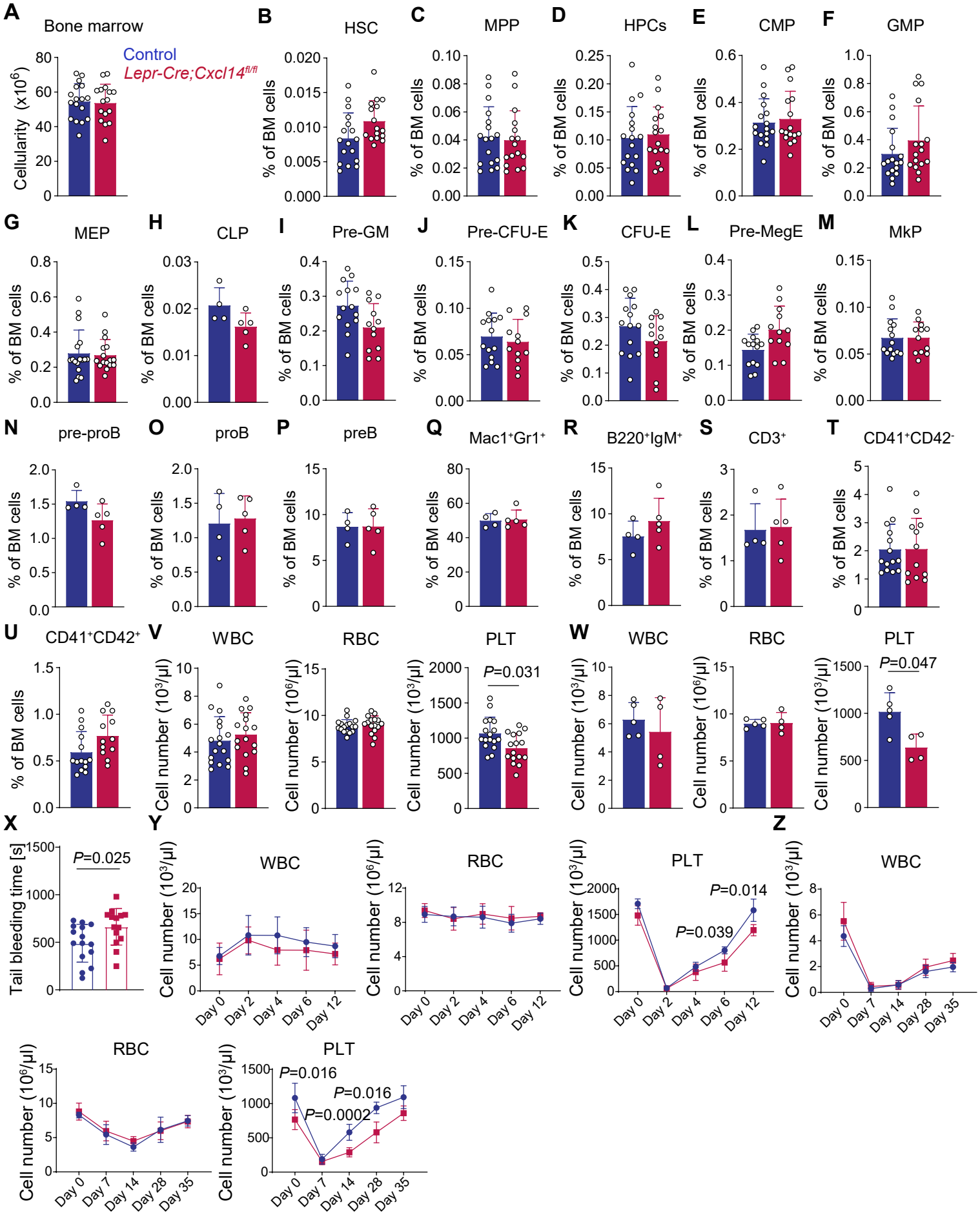
A
Bone marrow
Control
Lepr-Cre;Cxcl14fl/fl
Cellularity (x10^6)
B
HSC
C
MPP
D
HPCs
E
CMP
F
GMP
% of BM cells
G
MEP
H
CLP
I
Pre-GM
J
Pre-CFU-E
K
CFU-E
L
Pre-MegE
M
MkP
N
pre-proB
O
proB
P
preB
Q
Mac1+Gr1+
R
B220+IgM+
S
CD3+
T
CD41+CD42-
U
CD41+CD42+
V
WBC
RBC
PLT
Cell number (10^3/μl)
Cell number (10^6/μl)
P=0.031
W
P=0.047
X
Tail bleeding time [s]
P=0.025
Y
Day 0
Day 2
Day 4
Day 6
Day 12
P=0.014
P=0.039
Z
Day 7
Day 14
Day 28
Day 35
P=0.016
P=0.016
P=0.0002

Figure 3

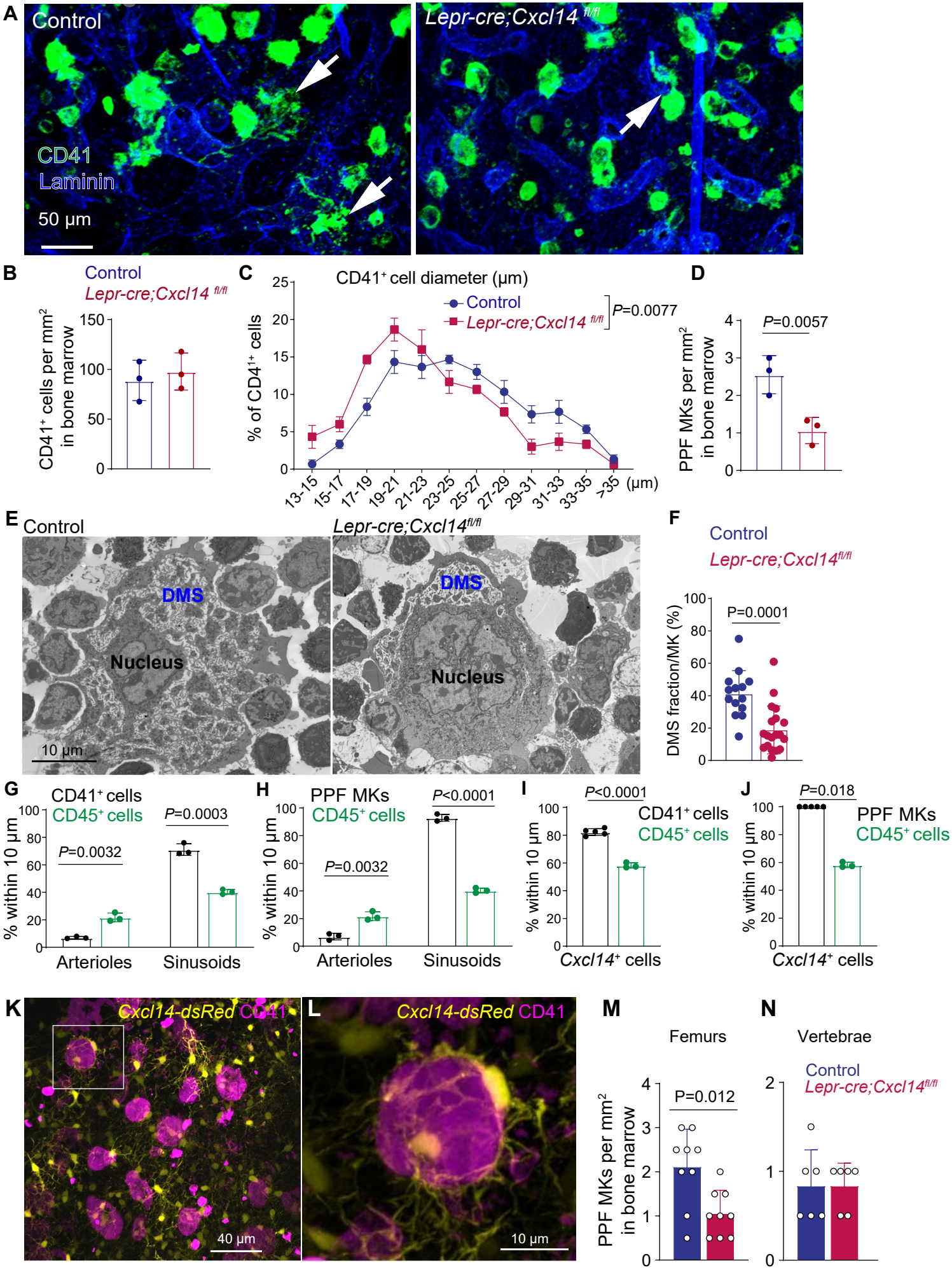
A
Control
Lepr-cre;Cxcl14 fl/fl
CD41
Laminin
50 µm
B
Control
Lepr-cre;Cxcl14 fl/fl
CD41+ cells per mm2 in bone marrow
C
CD41+ cell diameter (µm)
Control
Lepr-cre;Cxcl14 fl/fl
P=0.0077
% of CD41+ cells
13-15
15-17
17-19
19-21
21-23
23-25
25-27
27-29
29-31
31-33
33-35
>35
(µm)
D
P=0.0057
PPF MKs per mm2 in bone marrow
E
Control
Lepr-cre;Cxcl14fl/fl
DMS
Nucleus
10 µm
F
Control
Lepr-cre;Cxcl14fl/fl
P=0.0001
DMS fraction/MK (%)
G
CD41+ cells
CD45+ cells
P=0.0032
P=0.0003
% within 10 µm
Arterioles
Sinusoids
H
PPF MKs
CD45+ cells
P=0.0032
P<0.0001
% within 10 µm
Arterioles
Sinusoids
I
P<0.0001
CD41+ cells
CD45+ cells
% within 10 µm
Cxcl14+ cells
J
P=0.018
PPF MKs
CD45+ cells
% within 10 µm
Cxcl14+ cells
K
Cxcl14-dsRed CD41
40 µm
L
Cxcl14-dsRed CD41
10 µm
M
Femurs
P=0.012
PPF MKs per mm2 in bone marrow
N
Vertebrae
Control
Lepr-cre;Cxcl14fl/fl

Figure 4

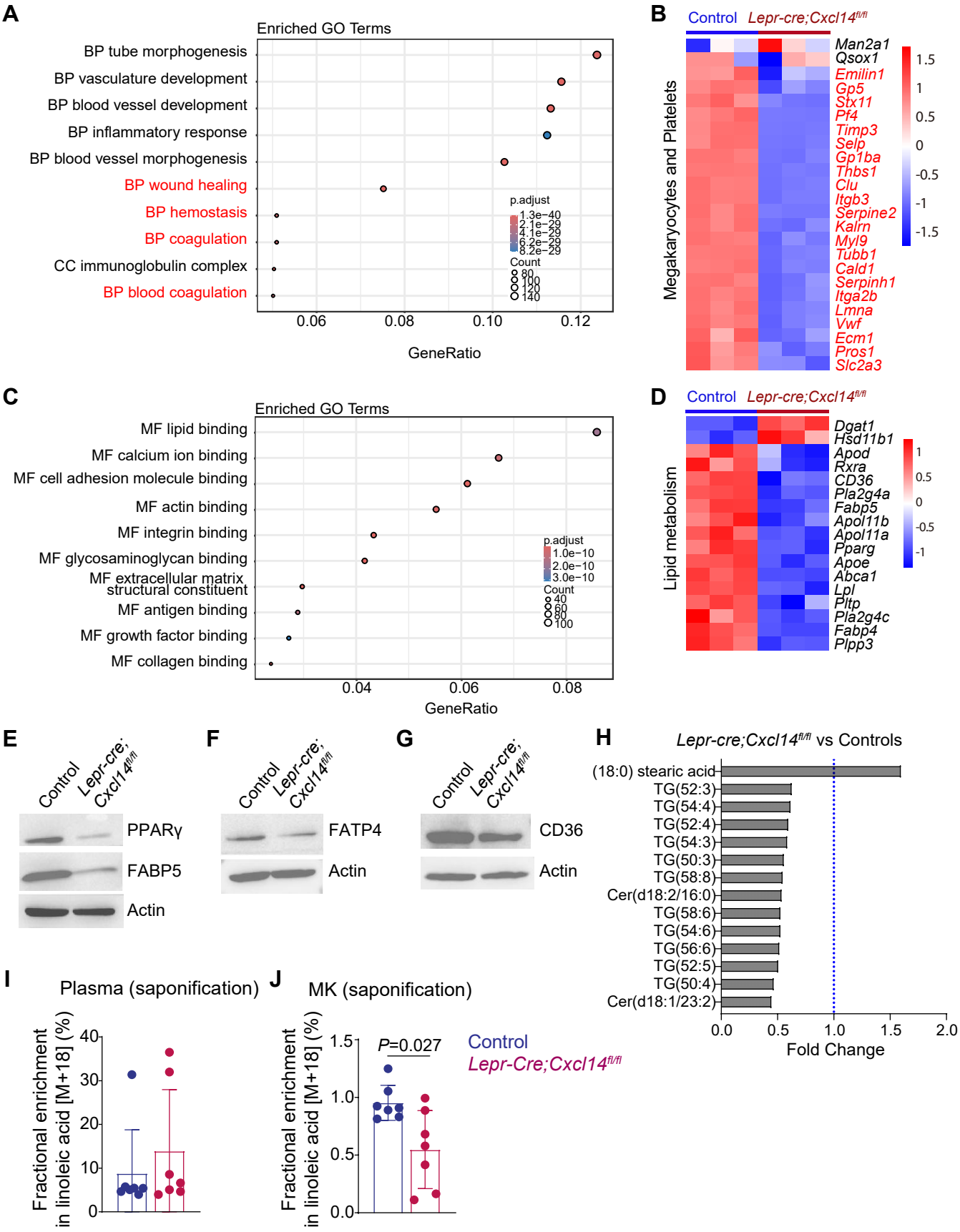
A
Enriched GO Terms
BP tube morphogenesis
BP vasculature development
BP blood vessel development
BP inflammatory response
BP blood vessel morphogenesis
BP wound healing
BP hemostasis
BP coagulation
CC immunoglobulin complex
BP blood coagulation
p.adjust
1.3e−40
2.1e−29
4.1e−29
6.2e−29
8.2e−29
Count
80
100
120
140
0.06
0.08
0.10
0.12
GeneRatio
B
Control
Lepr-cre;Cxcl14fl/fl
Megakaryocytes and Platelets
Man2a1
Qsox1
Emilin1
Gp5
Stx11
Pf4
Timp3
Selp
Gp1ba
Thbs1
Clu
Itgb3
Serpine2
Kalrn
Myl9
Tubb1
Cald1
Serpinh1
Itga2b
Lmna
Vwf
Ecm1
Pros1
Slc2a3
1.5
1
0.5
0
-0.5
-1
-1.5
C
Enriched GO Terms
MF lipid binding
MF calcium ion binding
MF cell adhesion molecule binding
MF actin binding
MF integrin binding
MF glycosaminoglycan binding
MF extracellular matrix structural constituent
MF antigen binding
MF growth factor binding
MF collagen binding
p.adjust
1.0e−10
2.0e−10
3.0e−10
Count
40
60
80
100
0.04
0.06
0.08
GeneRatio
D
Control
Lepr-cre;Cxcl14fl/fl
Lipid metabolism
Dgat1
Hsd11b1
Apod
Rxra
CD36
Pla2g4a
Fabp5
Apol11b
Apol11a
Pparg
Apoe
Abca1
Lpl
Pltp
Pla2g4c
Fabp4
Plpp3
1
0.5
0
-0.5
-1
E
Control
Lepr-cre; Cxcl14fl/fl
PPARγ
FABP5
Actin
F
Control
Lepr-cre; Cxcl14fl/fl
FATP4
Actin
G
Control
Lepr-cre; Cxcl14fl/fl
CD36
Actin
H
Lepr-cre;Cxcl14fl/fl vs Controls
(18:0) stearic acid
TG(52:3)
TG(54:4)
TG(52:4)
TG(54:3)
TG(50:3)
TG(58:8)
Cer(d18:2/16:0)
TG(58:6)
TG(54:6)
TG(56:6)
TG(52:5)
TG(50:4)
Cer(d18:1/23:2)
0.0
0.5
1.0
1.5
2.0
Fold Change
I
Plasma (saponification)
Fractional enrichment in linoleic acid [M+18] (%)
40
30
20
10
0
J
MK (saponification)
Fractional enrichment in linoleic acid [M+18] (%)
P=0.027
1.5
1.0
0.5
0.0
Control
Lepr-Cre;Cxcl14fl/fl

Figure 5

A

Diet	Carbohyrate (kcal%)	Fat (kcal%)	%SFA	%MUFA	%PUFA
Normal	70	10	24	30	47
HFD1	20	60	24	26	50
HFD2	20	60	32	36	32

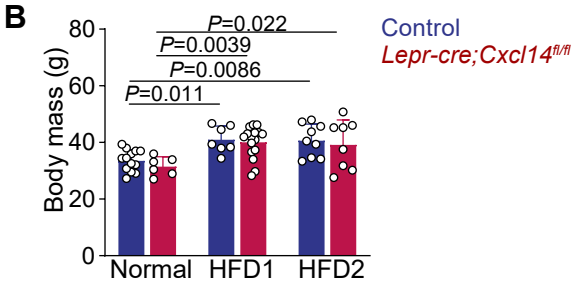

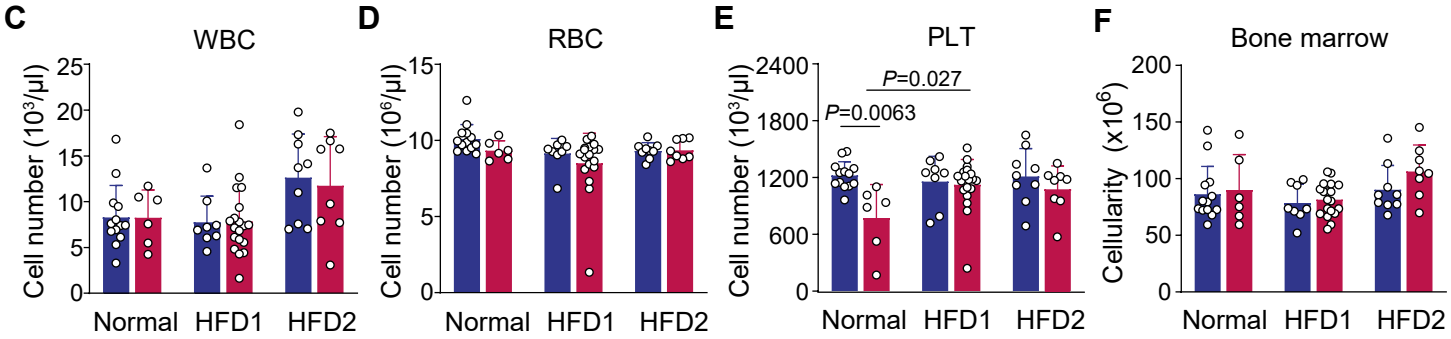

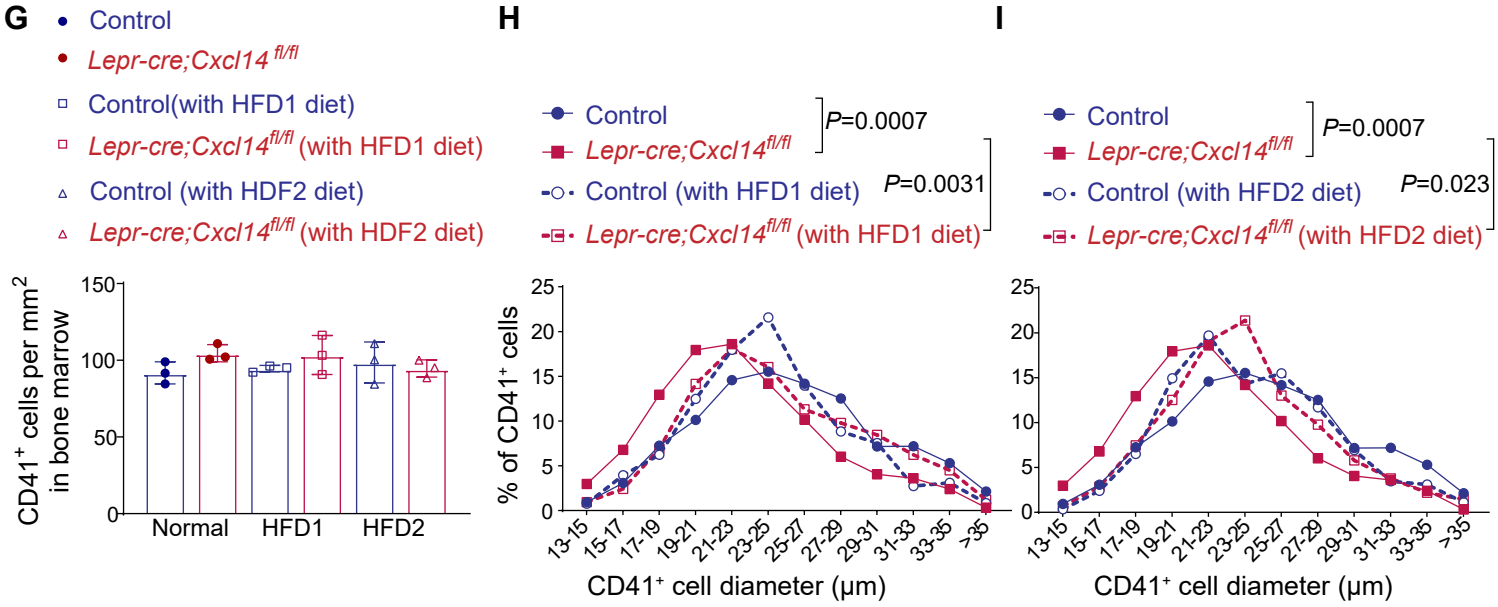

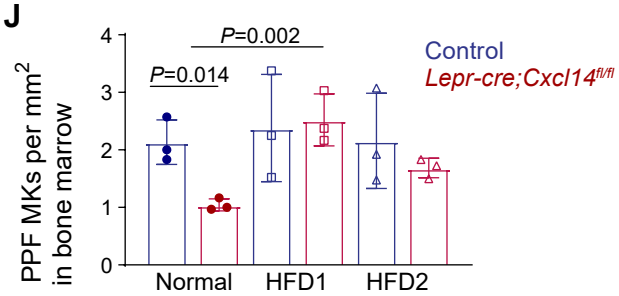

Figure 6

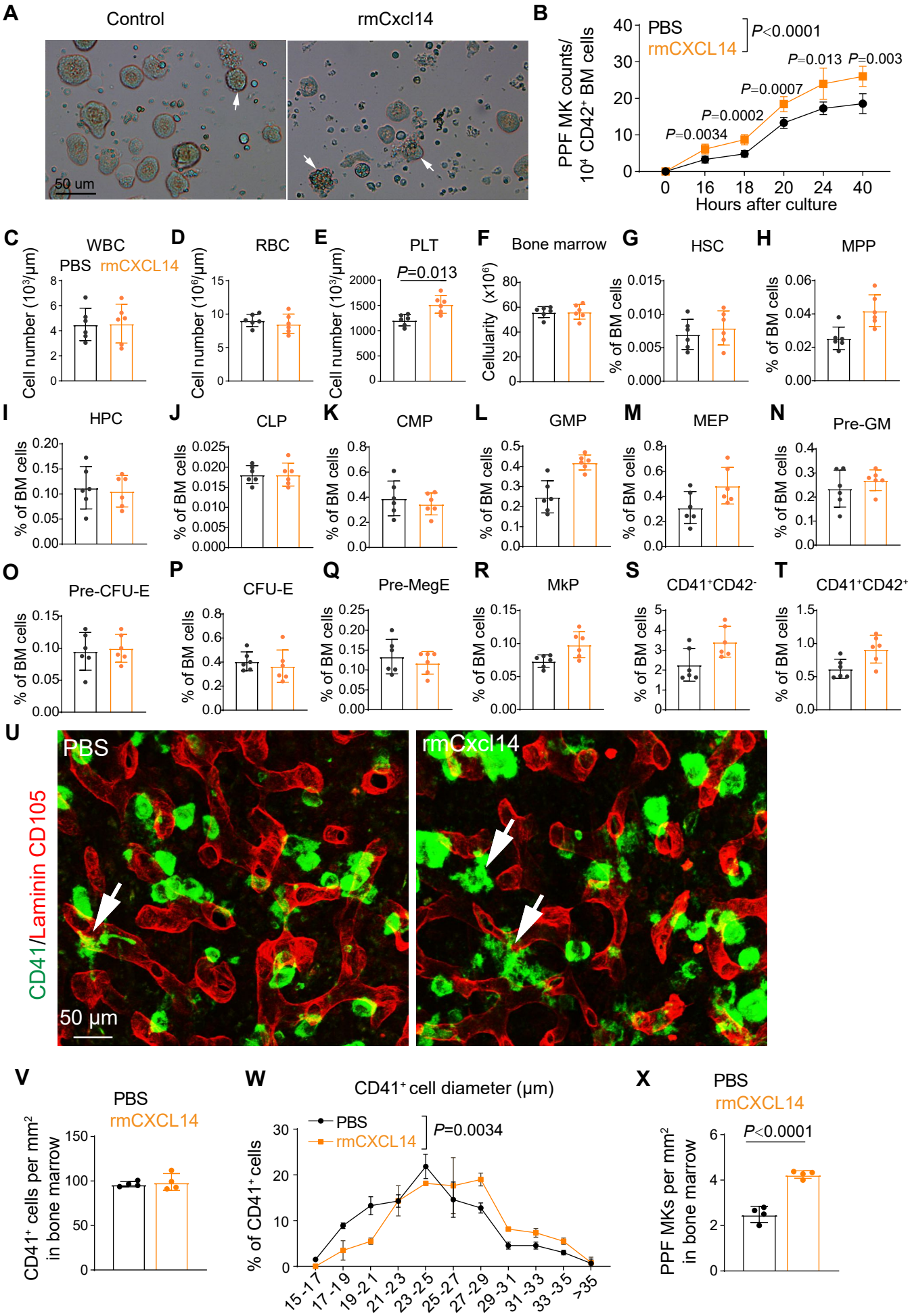
A
Control
rmCxcl14
50 um
B
PBS
rmCXCL14
P<0.0001
P=0.013
P=0.003
P=0.0007
P=0.0002
P=0.0034
PPF MK counts/ 10⁴ CD42⁺ BM cells
Hours after culture
C WBC
PBS rmCXCL14
Cell number (10³/μm)
D RBC
Cell number (10⁶/μm)
E PLT
P=0.013
Cell number (10³/μm)
F Bone marrow
Cellularity (x10⁶)
G HSC
% of BM cells
H MPP
I HPC
J CLP
K CMP
L GMP
M MEP
N Pre-GM
O Pre-CFU-E
P CFU-E
Q Pre-MegE
R MkP
S CD41⁺CD42⁻
T CD41⁺CD42⁺
U
PBS
rmCxcl14
CD41/Laminin CD105
50 μm
V
PBS
rmCXCL14
CD41⁺ cells per mm² in bone marrow
W
CD41⁺ cell diameter (μm)
PBS
rmCXCL14
P=0.0034
% of CD41⁺ cells
15-17
17-19
19-21
21-23
23-25
25-27
27-29
29-31
31-33
33-35
>35
X
PBS
rmCXCL14
P<0.0001
PPF MKs per mm² in bone marrow